Heliyon 10 (2024) e24629

Contents lists available at ScienceDirect

Heliyon

journal homepage: www.cell.com/heliyon

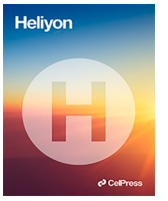

Research article

Study on motion behaviour of coal water slurry particles under vibration conditions

Yunfeng Bai *, Wenge Song, Qinju Liu

Guoneng Shendong Coal Group Co., Ltd. Yulin, Shaanxi, 719318, China

ARTICLE INFO

Keywords:
Coal water slurry (CWS)
Vibration
Motion behaviour
Computational fluid dynamics(CFD)

ABSTRACT

This study uses computational fluid dynamics (CFD) to simulate the motion behavior of coal-water slurry (CWS) particles under vibration conditions. Results show that without vibration, the coal particles settle to the bottom of the container due to gravity, forming distinct regions of low, transition, and high concentration. Under low vibration intensity, the slight energy activates particle motion and promotes settlement. Under high vibration intensity, violent reciprocating motion causes severe shaking and uncertainty, resulting in non-uniform particle distribution and back mixing. Particle velocity distribution is significantly influenced by vibration, with higher frequencies and amplitudes resulting in greater velocities. Additionally, particle pseudo-temperature is higher in the near-wall area due to collisions with particles and wall surfaces. Low frequency and amplitude promote particle settlement, increasing compactness in the bottom area and reducing concentration in the top area. The findings provide valuable insights into CWS behavior under vibration conditions, which can be used to optimize the design and operation of CWS handling and transportation systems.

1. Introduction

Coal is the most widely distributed and abundant fossil fuel in the world. According to the BP Statistical Yearbook of World Energy, coal accounted for about 27 % of global primary energy consumption in 2019 [1]. In recent years, with people's attention to the ecological environment and improving living standards, the clean and efficient use of coal has attracted more and more attention. It can not only meet our energy demand but also has a vital significance for realizing the clean use of coal and the goal of energy saving and emission reduction. Processing coal into CWS is one of the critical directions in developing clean coal technology. However, CWS is a kind of solid-liquid two-phase suspended fluid and a thermodynamically unstable system, which is prone to particle settlement and reduces its stability [2].

Coal water slurry (CWS) technology was developed in the 1970s as a branch of clean coal technology due to the impact of the oil crisis. CWS is formed by solid mixing of coal powder particles, water, and a few chemical additives [3]. It is a practical and cleaner coal-based oil fuel, and its preparation, storage, and transportation are entirely closed, preventing environmental pollution caused by traditional coal loading and transportation. Compared to coal gasification and liquefaction, CWS has low investment and cost, and it can be transported by tank, car, or pipe without causing environmental pollution during the storage process [4]. CWS has several clean properties. Its closed system prevents environmental pollution during the preparation, storage, and transportation processes [5].

* Corresponding author.
E-mail address: byf10029261@163.com (Y. Bai).

https://doi.org/10.1016/j.heliyon.2024.e24629
Received 17 August 2023; Received in revised form 2 November 2023; Accepted 11 January 2024
Available online 12 January 2024

Moreover, CWS can be transported long distances via pipelines, reducing transportation loss and solving the coal transportation problem [6]. Also, burning CWS can improve coal utilization efficiency, as its thermal efficiency can reach over 85 %, compared to 60 % for small and medium-sized coal-fired boilers [7]. CWS can also be atomized for combustion due to its water content, which lowers the flame center temperature by about 100 °C compared to fuel oil and gas [8]. This combustion process significantly reduces the emission of ammonia oxides and other pollutants [9].

CWS quality is essential and can be assessed based on the following aspects. First is the particle size, which varies depending on the type of CWS used. Fuel slurry has a maximum particle size of 300jm and a content below 74 μm of at least 75 %. Gasified slurry used in the chemical industry has a coal particle size below 1.4 mm and a content below 74 m of at least 50 % [10]. Coal particles within the coal-water slurry exhibit specific behaviors under various conditions, including their settling and motion patterns. Without vibration, these coal particles tend to settle to the bottom of the container due to gravity. This natural settling process results in distinct regions of low, transition, and high particle concentration within the slurry. Secondly, CWS concentration varies based on the coal grade and user demand, ranging from 50 % for lignite slurry to 75 % for high-rank bituminous coal [11,12]. Lignite, is considered a lower-grade coal due to its lower energy content and higher moisture content. In contrast, high-rank bituminous coal is known for its greater energy density and lower moisture content. The concentration of CWS can be tailored to match the characteristics of the coal being used. For lignite, a concentration of around 50 % might be suitable, ensuring that the resulting slurry can effectively transport the lower energy content while maximizing its fluid properties. On the other hand, high-rank bituminous coal, which has a higher energy content, can be mixed into a slurry with a concentration of approximately 75 % to efficiently transport the higher energy load. Thirdly, rheological properties require CWS to have good fluidity and "pseudoplastic" fluid properties whose viscosity decreases with the increase of shear rate [13]. Fourth is the stability, which is important to maintain uniform and stable properties, as CWS is a thermodynamically unstable system that can separate the solid and liquid phases [14]. Static stability and dynamic stability are two forms of CWS stability, and while the Turbiscan Lab stability analyzer is useful in evaluating static stability, dynamic stability remains unclear [15,16]. To study the dynamic stability of CWS under vibration conditions for transportation and distribution, this paper focuses on the motion behavior of coal particles in CWS. However, due to the high concentration and opacity of CWS, observing the settling characteristics of coal particles in CWS can be challenging [17].

In recent years, with the development of computer technology, it has become possible to use Computational Fluid Dynamics (CFD) to simulate the actual flow behaviour of a fluid in a small-scale device [18]. Based on this, the current dominant CFD software, Fluent 16.0, is used in this paper to simulate the motion behaviour of coal particles in CWS under vibration conditions.

2. Methodology

Computational Fluid Dynamics(CFD) is a branch of computational mechanics. At first, CFD was mainly applied in aviation [19]. After decades of development and improvement, it has penetrated many engineering fields, including aviation, aerospace, shipbuilding, and the chemical industry [20]. Compared with fluid dynamics under experimental conditions, it has the advantages of less investment, faster calculation, complete information, and not being limited by model size, so it is a powerful tool for studying fluid dynamics.

At present, the discrete methods of governing equations used in CFD calculation mainly include three forms: the finite difference method (FDM), the finite element method (FEM) and the finite volume method (FVM) [21]. In numerical calculation, the finite volume method is the most commonly used. This method is also called the control volume method. Currently, the most commonly used commercial CFD software, Fluent, is developed based on the algorithm programming of the finite volume method [22]. It has a convenient development platform and contains a variety of complex fluid flow model equations. At the same time, users can also use C language to compile the User Defined Function (UDF) file according to the actual research problems to realize the numerical simulation calculation of various complex fluid flow problems [23]. Based on this, this chapter mainly uses the Fluent 16.0 platform to calculate and solve the numerical simulation process.

2.1. Selection of liquid-solid two-phase flow model

The settlement of coal particles in CWS is a typical liquid-solid two-phase flow, in which the continuous phase is water, and the discrete phase is coal particles [24]. This section from the CWS in the specific characteristics of liquid-solid two-phase flow, the body fit through the particle phase flow and determine various external expression in the model, based on Euler's method of coal-water slurry in liquid-solid two-phase flow dynamic two-fluid model.

In computational fluid dynamics, the fluid-particle two-phase flow system is generally divided into particle and fluid phases. Depending on the treatment methods of the particle phase and fluid phase, they can be divided into the continuum model, discrete particle model and pseudo particle model.

2.2. Numerical solution method

2.2.1. Establishment of the geometric model

The container used in this study for CWS experiments is a cylindrical body with an inner diameter of 40 mm and a height of 100 mm. Since the size of the cylinder is small, the grid geometry model is constructed to be consistent with the actual size of the container. Although a three-dimensional model can improve the calculation accuracy, it requires a large amount of computation time. Therefore, in this study, the three-dimensional container model was simplified for ease of computation during the later simulation process. When

simplifying the three-dimensional container model, two assumptions need to be satisfied, namely: the coal particles for fluidization analysis are uniform spheres and the distribution of coal particles in the CWS is uniform throughout the container. Additionally, Lettieri et al. also found that two-dimensional models and three-dimensional models have good consistency in simulation results. Based on the above assumptions and previous research results, this study simplified the calculation domain into a 40 mm × 100 mm two-dimensional geometric body. Such processing not only greatly saves computation time but also reflects the motion characteristics of the liquid-solid two-phase in the CWS under vibration conditions.

2.2.2. Grid division

After establishing the geometric model, the next step is to divide the calculation domain of the model into grids. Grid division is a crucial pre-processing step for numerical simulations because the quality of the grid directly affects the accuracy of the numerical simulation results. For two-dimensional problems, the commonly used grid models in Fluent are triangles, quadrilaterals, or mixed grids [25]. Considering that dynamic layering is used as the method to generate dynamic grids in this simulation, which is a simple linear motion that removes one layer of grids at a time when compressed and adds one layer of grids at a time when stretched, it is only suitable for structured grids such as quadrilaterals or hexahedrons. Therefore, in this simulation, a quadrilateral grid is used to divide the calculation domain into grids. The ANSYS ICEM software is used to divide the calculation domain into grids, with regular quadrilateral grids being used for the grid shape. The total number of grids is 16,000, and each grid size is 0.5 mm × 0.5 mm.

2.2.3. The setting of physical parameters and boundary conditions

The physical properties of the two-phase liquid-solid system were defined, and the particles were pseudo-fluidized. Then, the boundary conditions of the model were defined. Since the container was closed during the vibration, all walls of the model were set as stationary walls.

By developing a UDF program, a sine wave vibration was added to the CWS cylinder model, and dynamic grid technology was employed to implement the cylinder model's vibration, with initialization of both the solid and liquid phases. Since the grid partition for this simulation is made up of regular quadrilateral shapes, the dynamic layering model was chosen for the parameter model of grid updating. Regarding the selection of grid motion, the UDF provided three types: Rigid Body, Stationary, and Deforming [26]. Considering that the simulated coal-water slurry container is a cylindrical body that can be treated as a rigid body, the Rigid Body form was chosen for the grid motion.

2.2.4. Discretization of the governing equations

When discretizing the governing equations, the basic idea is to divide the fluid region into many non-identical control volumes, integrate the differential equations to each control volume, and obtain a set of discrete equations to solve for the approximate solution of the desired variable [27]. Commonly used discrete methods in Fluent include the first-order upwind, second-order upwind, central differencing, and QUICK schemes. In this simulation, because regular quadrilateral grids are used, the fluid motion and grid almost align in a straight line. Moreover, the first-order upwind scheme ensures that the coefficients are always non-negative during calculation and avoids physically unreasonable solutions, making it the chosen method for discretizing the governing equations.

2.2.5. Selection of solution method

CWS can be regarded as an incompressible fluid. When solving for the motion of incompressible fluids, the difficulty in pressure

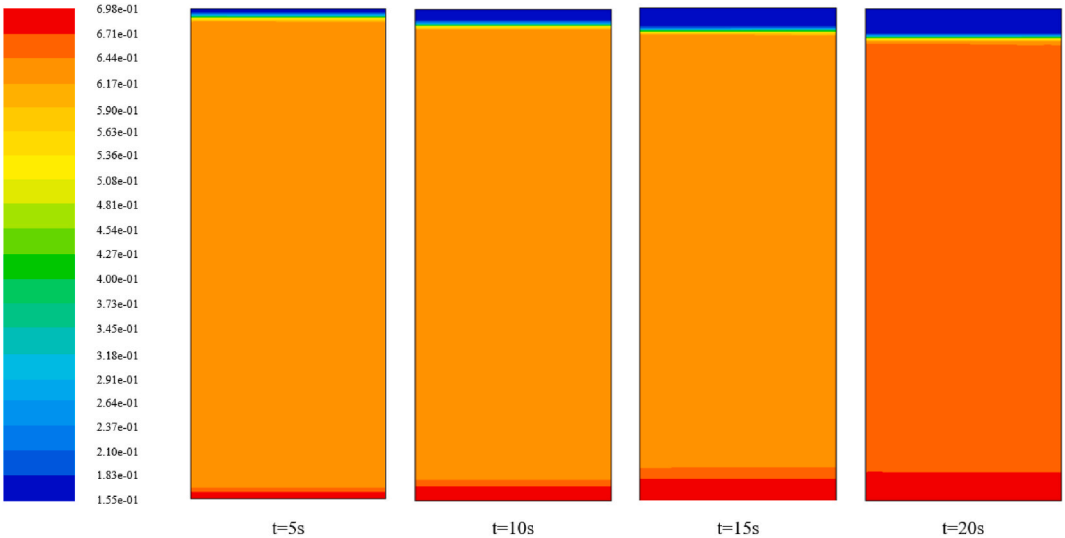

Fig. 1. Particle concentration in CWS at different times when f = 0Hz and A = 0 mm.

calculation arises from the lack of a separate pressure equation in the incompressible fluid flow field [28]. Coupling can only be achieved through the continuity equation. Currently, the most widely used method for flow field calculations in engineering is the pressure correction algorithm, which has various implementation forms. The most common one is the semi-implicit algorithm based on pressure coupling, namely the SIMPLE algorithm. In this simulation, the solution method used is the SIMPLE algorithm based on pressure-velocity coupling.

3. 3. simulation results and analysis

3.1. Settlement characteristics of CWS under different vibration conditions

When no vibration is added, the sedimentation of coal particles in CWS is mainly affected by gravity. When a vertical sinusoidal vibration is applied to the cylinder, the motion of coal particles can be regarded as being dominated by gravity and excitation force. Under the condition of low frequency and low amplitude, the excitation force received by coal particles is not enough to overcome the action of gravity, but with the increase of amplitude and frequency, the excitation force may gradually dominate. Therefore, the settling process of CWS may show different characteristics under different amplitude and frequency conditions.

Fig. 1 shows the concentration distribution of CWS at different moments under static conditions (f = 0Hz, A = 0 mm). As seen in Fig. 2, due to gravity only, the coal particles in the CWS gradually settled to the bottom of the container. And the CWS concentration showed regular stratification along the height of the cylinder and presented three distinct regions: the low concentration region at the top of the cylinder, the transition region in the middle of the simplified character and the high concentration region at the bottom of the cylinder.

Fig. 2 shows the simulated concentration distribution of CWS at different times under low frequency (f = 10Hz) and low amplitude (A = 0.25 mm). It can be seen from the figure that when low excitation force is applied, the settlement of CWS still mainly occurs at the top and bottom of the container, and the stratification phenomenon is still apparent. With the increase of simulation time, the coal particles at the top gradually settle to the bottom of the container. Resulting in a gradual decrease in the concentration of coal particles at the top and a gradual increase in the concentration of coal particles at the bottom. Due to the low vibration intensity, the exciting force of particles is not enough to overcome gravity, and the small vibration energy may loosen the particle group and promote its settlement under gravity. Compared with Fig. 1, at this time, the boundary between layers of CWS concentration is not as apparent as under static conditions but shows a gradual concentration process.

Fig. 3 shows the simulated concentration distribution of CWS at different times under high frequency (f = 100Hz) and high amplitude (A = 1.25 mm). As seen from Fig. 3, under this condition, the concentration of coal particles still presents the characteristics of high concentration at the bottom and low concentration at the top. However, due to the high vibration intensity and the severe shaking and uncertainty of the container, the coal particles did not uniformly fall along the axial direction of the simplified character. However, back mixing appeared up and down, especially in the top and bottom areas, which was more prominent. CWS concentrations are identified and translated into completely different characteristics along the network in the near-wall and central regions of the simplified characters. Due to the high vibration intensity, the exciting force of particles is much greater than the effect of gravity. The reciprocating motion caused by sinusoidal vibration may be the leading cause of this phenomenon.

It can be found from the concentration distribution diagram under the above three conditions that the CWS concentrations at different height positions show significantly different characteristics under low and high vibration intensification. Moreover, the

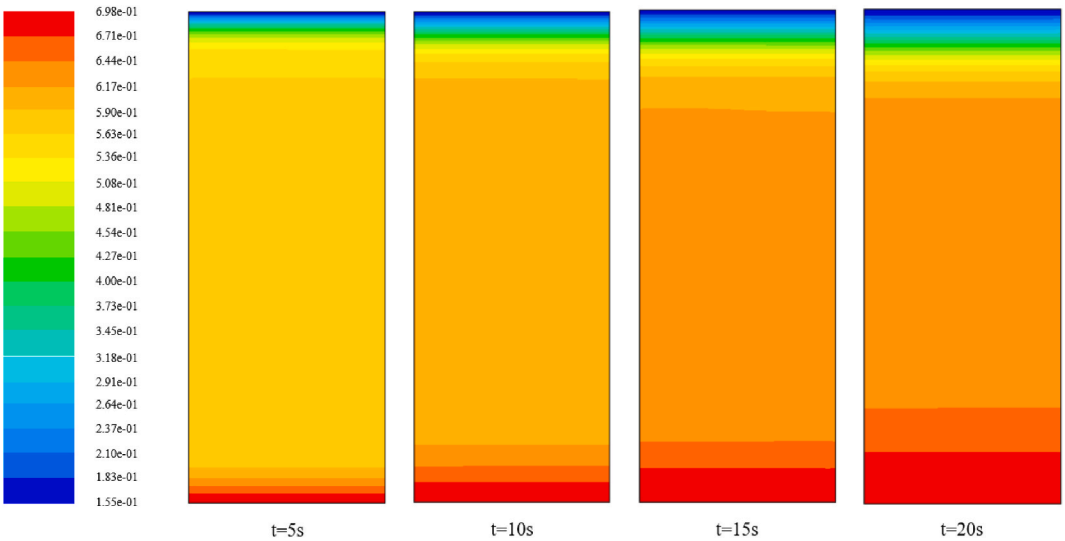

Fig. 2. Particle concentration in CWS at different times when f = 10Hz and A = 0.25 mm.

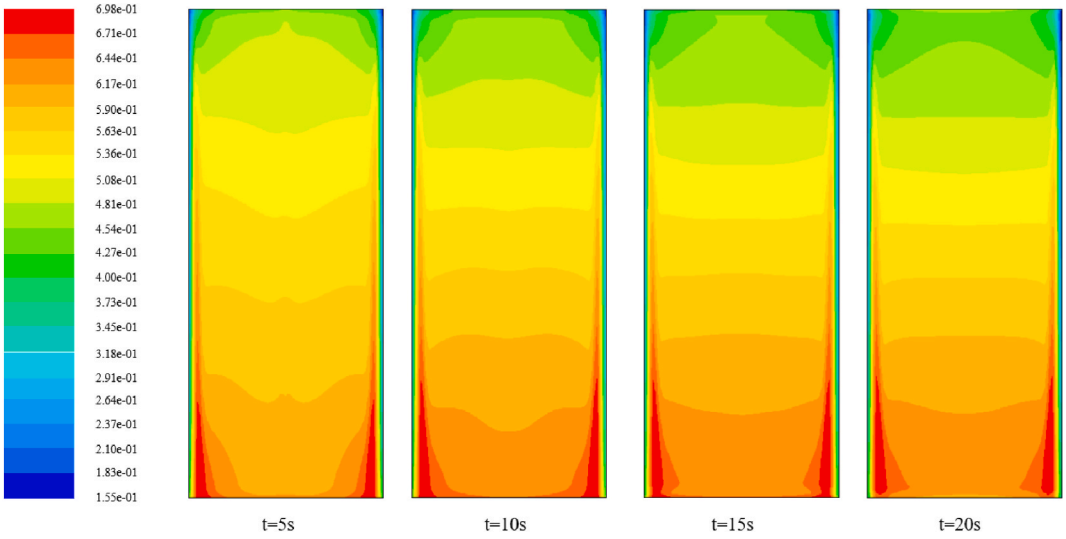

Fig. 3. Particle concentration in CWS at different times when f = 100Hz and A = 1.25 mm.

concentrations in the simplified wall and the central area also differ significantly under high vibration intensification. Therefore, three different height positions y = 5 mm (bottom), y = 50 mm (middle) and y = 95 mm(top), were selected to study the concentration distribution at the 20s. Fig. 4 shows the radial distribution of CWS concentrations at different heights under different vibration parameters. It can be seen from Fig. 4(a) and (b) that under static and low vibration intensity conditions, the concentration of CWS at different heights does not change along the simplified radial direction. When y = 5 mm and y = 50 mm, the volume fraction is roughly similar. At the height of y = 95 mm, the volume fraction without vibration is approximately 0.4, while under the condition of low vibration, the volume fraction is approximately 0.3, indicating that low frequency and low amplitude can promote the settlement of

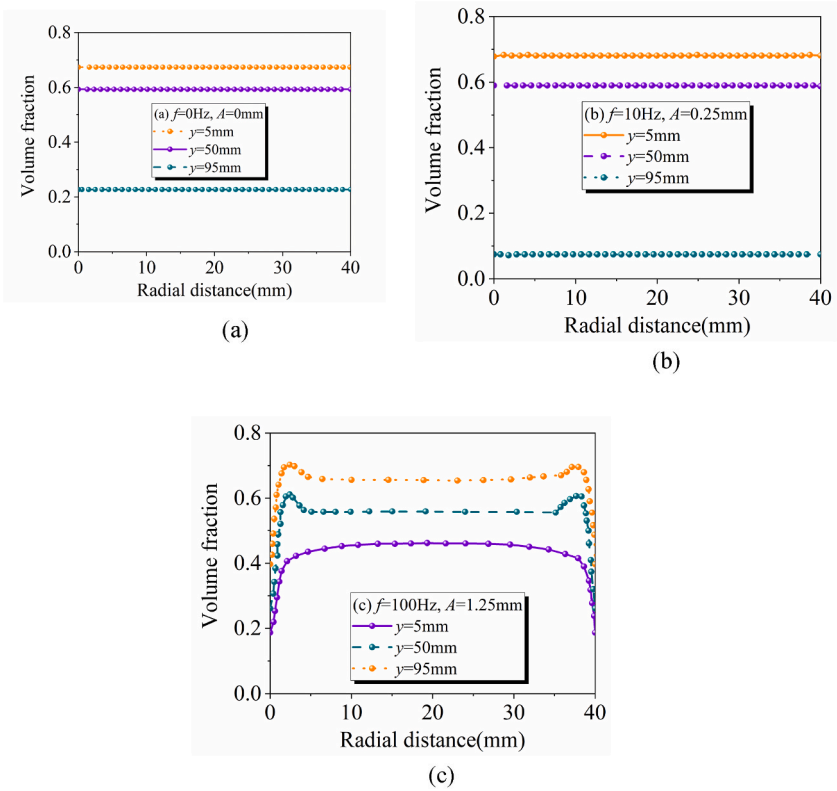

Fig. 4. Radial distribution of the volume fraction of the Cws at different heights under different vibration conditions.

coal particles in the top area. The lower vibration energy can activate the motion of coal particles under gravity, thus promoting the settlement of coal particles. However, at high vibration intensity (Fig. 4(c)), there is a significant difference in coal particle concentration between the near wall and central areas. At y = 95 mm, the volume fraction is roughly 0.53, indicating that high frequency and high amplitude are not conducive to particle settlement. Vital vibration energy will increase the degree of looseness between particles, accelerate the motion speed of particles, and reciprocate sinusoidal motion. It will lead to a violent collision between particles, thus hindering the settlement process of particles to a certain extent.

In addition, in order to better reflect the changes of CWS concentration at different locations under different vibration conditions, three different height locations, and the change of its concentration over time was monitored. The results are shown in Figs. 5–7. As can be seen from Fig. 5(a), when vibration is not added, the time evolution curves of concentrations at three different height positions in the near-wall and central regions are basically similar. The concentration of CWS at the bottom (y = 5 mm) gradually increases with time, caused by the settlement of the particles above. In the middle position (y = 50 mm), the concentration of CWS increases only slightly. At y = 95 mm, the concentration of CW-water increases slightly at first, which may be caused by the deposition of particles in the top region (y > 95 mm). However, due to the settlement of particles in the top region, the concentration at this position increases, so the compressed coal particles move further to the bottom, which shows that the concentration decreases rapidly after the simulated 16s.

Fig. 5(b) shows the time evolution curve of CWS concentration at different height positions under low frequency and low amplitude conditions. It can be seen from the figure that, at low vibration intensity, the time evolution curve of the concentration in the near-wall region and the central region is still similar. Compared with the static condition, the concentration at the height of y = 5 mm began to increase significantly after 2s. In comparison, the phenomenon occurred after 10s under the static condition, indicating that the slight vibration was favourable for the coal particles to settle to the bottom of the simplified character. The addition of vibration can make the particle layer lose and weaken the hindrance effect of the bottom particles on the settlement of the upper particles, which is more conducive to the settlement of coal particles at the bottom of the container. At the height of y = 50 mm, the change of its concentration with time is different from that under the static condition. However, at the height of y = 95 mm, the particle concentration decreases obviously after 2s. Especially at the 20s, the particle volume fraction decreases to 0.3, which is only about 0.4 when no vibration is added. This indicates that the settlement of coal particles in CWS under low vibration intensity is similar to that under static conditions, and slight vibration can accelerate the settlement process of coal particles under gravity.

Fig. 7(a) shows the time evolution curve of CWS concentration at different positions under the condition of high frequency and high amplitude. It can be seen from Fig. 7 (b) that in the central region, the variation trend of CWS concentration at the height of y = 5 mm and y = 50 mm over time is similar to Figs. 5 and 6. However, at y = 95 mm, although the concentration decreases very early, the volume fraction only drops to about 0.55 at the 20s. This shows that, on the one hand, the addition of vibration can promote the settlement of coal particles in the bottom area. On the other hand, the reciprocating motion caused by vital vibration energy and sinusoidal vibration will also cause back mixing or backflow of some coal particles, which is the main reason for the high concentration of coal particles in the top layer under high vibration intensity. In addition, it can be seen from Fig. 7(a) that in the area near the wall, the change of coal particle concentration over time shows different characteristics. Under high vibration intensity, vital vibration energy can push coal particles in the cylinder to move up and down, reciprocating. However, due to the obstruction effect of the wall surface on particle movement, the particles in the central area move faster. However, the movement speed of particles in the near-wall area is slow, which pushes some particles in the central area to move to the left and right direction, resulting in the phenomenon that the concentration of coal particles in the near-wall area is higher than that in the central area at y = 5 mm and y = 50 mm. However, due to the obstruction effect of the top cover of the cylinder, the further upward movement of coal particles is prevented, causing some coal particles to accumulate in the top area, which may be the main reason that the concentration of coal particles in the central area is higher than that near the wall area at the height of y = 95 mm.

In order to study the experimental phenomena in depth and to strengthen the mechanism analysis, this paper also simulates the force analysis of microscopic particles under different vibrational conditions (see Table 1). This analysis will investigate the forces acting on individual particles, such as gravity, inter-particle forces and vibrational forces. Understanding the interaction of these forces

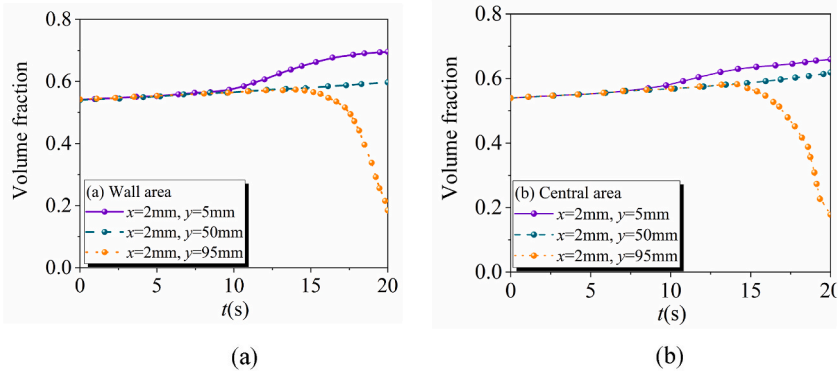

Fig. 5. Time evolution of the volume fraction of the cws at different locations under the condition of f = 0Hz and A = 0 mm.

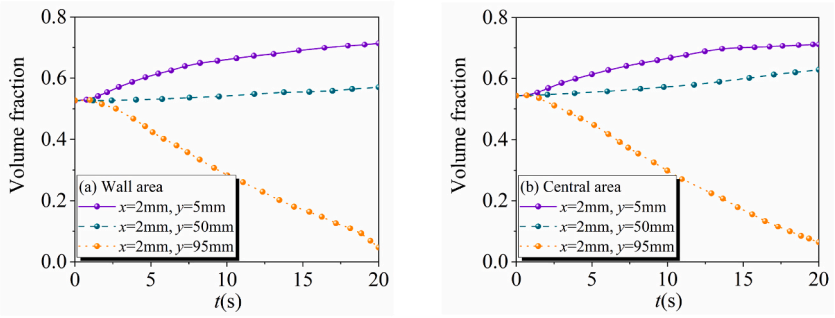

Fig. 6. Time evolution of the volume fraction of the CWS at different locations under the condition of f = 10Hz and A = 0.25 mm.

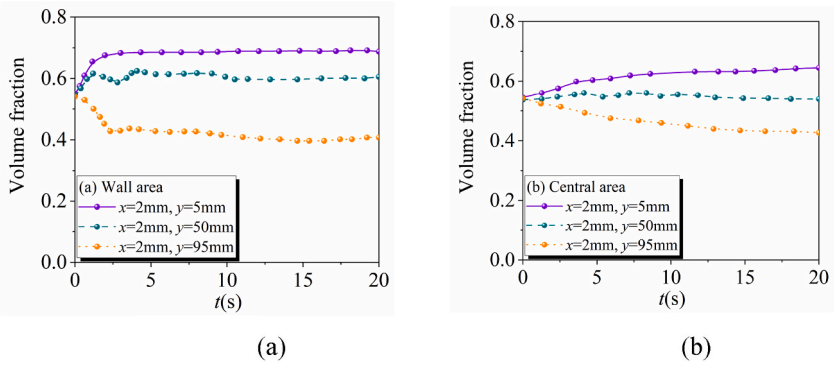

Fig. 7. Time evolution of the volume fraction of the CWs at different locations under the condition of 100Hz and A = 1.25 mm.

can provide insight into the settling process.

In this micro-particle force analysis, we consider the effects of gravity, particle-particle interaction forces (which can be attractive or repulsive depending on distance and charge), and vibration forces. Gravity encourages particles to settle downward, particle-particle interaction forces can be either attractive or repulsive based on distance and charge conditions, and vibration forces impact particle positions, with the direction and amplitude of vibration determined by vibration conditions. These forces collectively act on individual particles, influencing their microscale behaviors.

3.2. Effect of vibration on particle velocity

3.2.1. Effect of vibration on particle velocity at different heights

The addition of sinusoidal vibration makes the particles in the simplified characters subject to the double action of gravity and excitation force, which results in the change of the axial velocity of the particles with the change of vibration parameters. Fig. 8(a) shows the radial distribution of particle axial velocity at 10s at different heights without vibration. Only under the action of gravity, the motion velocity of particles is small on the whole, no more than 0.007 m/s. When y = 5 mm, the particle axial velocity does not change with the radial position. However, in the top layer of y = 95 mm, the motion velocity of particles in the central region is higher, while that of particles in the wall region is smaller. This may be because the wall surface is a non-slip boundary, which will have a certain hindrance to the movement of particles in the process of particle settlement. Due to the high particle concentration, the settlement of the upper particles compresses the downward movement of the lower particles as a whole. Therefore, the axial velocity of the particles at y = 5 mm basically does not change with the radial direction.

Table 1
Analysis of forces on microscopic particles under different vibrational conditions.

Force	Nature and Direction	Magnitude (Newtons)	Influence
Gravity	Vertically downward, proportional to particle mass	0.02	Promotes particle settling downward
Particle-particle interaction force	Mutual attraction or repulsion, depends on distance and charge	0.01	Causes particles to approach or move away from each other
Vibration force	Vibration direction and amplitude depend on vibration conditions	0.015	Influences particle position under vibration conditions

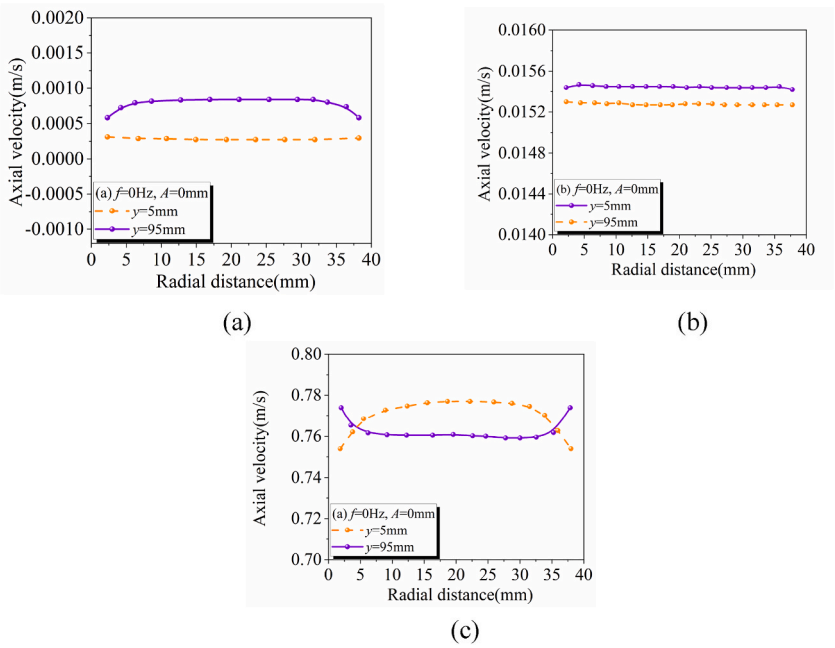

Fig. 8. Distribution of the axial velocity of the particles at different heights.

Fig. 8 (b) shows the radial distribution of the axial velocity of particles at different heights at 10s under low vibration intensity (f = 15Hz, A = 0.25 mm). As can be seen from the figure, the movement speed of particles in the bottom region is significantly higher than that in the top region, which is exactly the opposite of the case without vibration. This is because when vibration is applied, the particles at the bottom of the simplified character are the first to be affected by vibration, and the vibration energy is further transferred to the top particles through the collision of particles. As a result of energy dissipation, the speed of particles in the top region is lower. At the same time, it can be found that under this condition, the axial velocity of particles at different heights tends to be equal in the radial direction, which may be because the addition of vibration will activate the movement of particles in the near-wall area, making the axial motion of particles at different radial positions more stable. According to the, at 10s, the motion velocity generated by the excitation force is 0.0158 m/s. However, because the particles are also affected by gravity and part of the energy is dissipated due to particle collision, the motion velocity of the particles in the cylinder is lower than 0.0158 m/s.

Fig. 8(c) shows the radial distribution of axial velocity of particles at 10s at different heights under high vibration intensity (f = 100Hz, A = 1.25 mm). As can be seen from the figure, under high vibration intensity, the axial velocity of particles still presents the characteristics of higher velocity at the bottom and lower velocity at the top. However, under this condition, the axial velocity of particles at different heights changes with the radial direction. At the height of y = 5 mm, the movement velocity of particles in the central region is higher than that in the near-wall region. At y = 95 mm, the opposite is true. Although the application of vibration can activate the movement of particles in the near wall area, due to the large vibration energy, particles move faster under the action of excitation force, and the collision between particles and the wall surface in the near wall area and other factors will inevitably hinder the movement of particles in the area. Due to the obstruction effect of the top cover of the cylinder, particles accumulate in the area

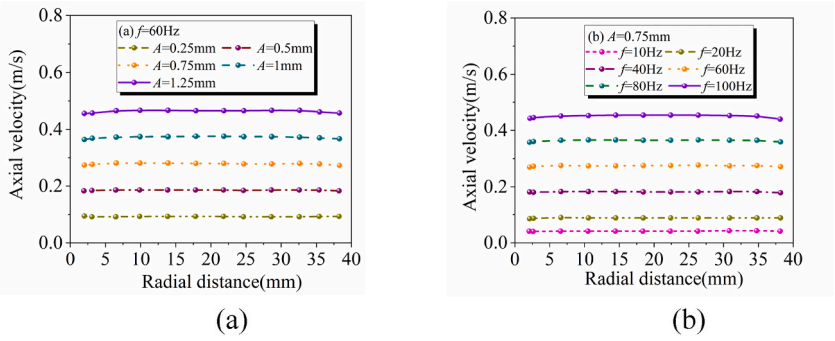

Fig. 9. Distribution of the axial velocity of the particles with different vibration parameters (a) with vibration amplitude (b) with vibration frequency.

with a height of y greater than 95 mm, resulting in a phenomenon that the concentration of particles in the central area is higher than that in the near wall area (Fig. 4(c)). The collision of particles in the central area is more intense, which may be the main reason why the movement speed of particles in the central area is lower than that in the near wall area at the height of y = 95 mm.

3.2.2. *Influence of different vibration parameters on particle velocity*

Fig. 9 shows the radial distribution of particle axial velocity at 10s under different vibration parameters at a height of y = 5 mm. As can be seen from Fig. 9(a), when the frequency is the same, the particle velocity as a whole increases with the increase of amplitude. At low amplitude, the particle velocity does not change along the radial direction. With the increase of amplitude, the particle velocity gradually presents the characteristics of large in the middle and small at both ends. This may be due to the fact that when the amplitude is higher, the vibration intensity is larger, the particles are excited by larger force, and the motion speed is faster. However, in the near-wall area, because the wall surface is a non-slip boundary, the motion of particles will be hindered to a certain extent. At the same amplitude (Fig. 9(b)), with the increase of frequency, the vibration intensity increases and the particle motion velocity also increases gradually. When the frequency is higher, the particle velocity in the central region is also greater than that in the near-wall region. With the decrease of frequency, the particle velocity tends to be equal in the radial direction. Through the above analysis, it can be seen that low frequency and low amplitude will make the particle velocity distribution more uniform in the radial direction, that is to say, low vibration intensity will make the particle velocity at different radial positions more stable, while high vibration intensity will cause the particle velocity at different radial positions to be uneven distribution, but the motion velocity is still affected by vibration parameters on the whole.

3.3. *Characteristics of particle pseudo-temperature distribution*

Particle pseudo-temperature is also known as particle pulsation kinetic energy, which can reflect the intensity of collisions between particles. The higher the particle pseudo temperature is, the faster the particles move, and the more violent the collision between particles is.

3.3.1. *Influence of different vibration parameters on particle pseudo-temperature*

Fig. 10 shows the distribution of particles' pseudo temperatures along the height of the cylinder at different radial positions under the conditions of static (f = 0Hz, A = 0 mm), low frequency and low amplitude (f = 10Hz, A = 0.25 mm) and high frequency and high amplitude (f = 100Hz, A = 1.25 mm), respectively. As can be seen from Fig. 10(a), only under gravity, particle collisions mainly occur in the top region due to the slight motion velocity of particles. Combined with Fig. 8(a), it can be seen that the movement speed of particles in the top region is significantly higher than that in the bottom region, which is the main reason for the high temperature of

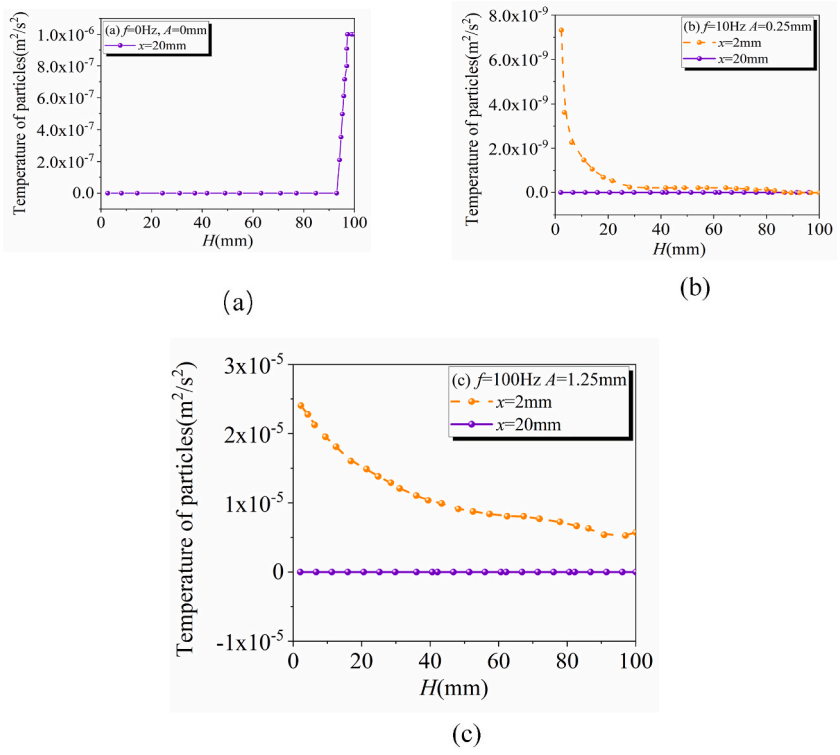

Fig. 10. Distribution of the granular temperature under different vibration parameters.

particles in the top region. However, in the case of low vibration intensity (Fig. 10(b)), the temperature of particles in the bottom area is relatively high, and the pseudo-temperature of particles decreases sharply with the increase in height. When vibration is applied, the particles at the bottom of the simplified character are the first to be affected by vibration, and the vibration energy is further transferred to the top particles through the collision of particles, resulting in a lower motion speed of the top particles (Fig. 9(b)). Secondly, due to the sedimentation of particles, the concentration of the bottom particles is higher, and the chance of particle collision is more significant. Therefore, the collision of the bottom particles is more intense than the top particles. Moreover, as coal belongs to organic matter, with the increase in height, the agglomeration tendency among coal particles increases and the collision return coefficient of particles decreases due to the dissipation and reduced vibration energy during transmission. In addition, the temperature of particles at x = 2 mm is significantly higher than that at x = 20 mm. This is because in the area near the wall at x = 2 mm, due to the non-slip characteristics of the wall, in addition to the collision between particles, particles will also collide with the wall. With the further increase of vibration intensity (Fig. 10(c)), the pseudo-temperature of particles increases rapidly. Compared with the low vibration condition, the temperature of particles in the near wall area is still higher than that in the central area. However, the decreasing trend of particle temperature at x = 2 mm with height slows down significantly, and the pseudo particle temperature at y = 100 mm is still higher, indicating that the collision of particles in the top area is still very intense under the high vibration intensity.

3.3.2. *Effect of different amplitudes and frequencies on particle pseudo-temperature distribution*

Fig. 11 shows the variation of particle pseudo temperature at different radial positions with the height of the cylinder at different amplitudes. As can be seen from the figure, the pseudo-temperature of the particle increases gradually with the increase of the amplitude. In the radial position, the pseudo-temperature of the particles near the wall varies significantly with the height, and its value is higher than that in the central area. When the amplitude is low at the top of y = 100 mm, the temperature difference between the particles at x = 2 mm and x = 20 mm is small. With the increase of amplitude, the temperature difference also increases gradually.

Fig. 12 shows the variation of particle pseudo temperature with height under different frequency conditions. It can be found that the variation law with frequency is similar to that with amplitude. When the amplitude or frequency is higher, the vibration intensity is more significant, the particles are excited by force is larger, the speed of particle movement is faster, and the intensity of the collision between particles and between particles and the cylinder wall surface increases. On the other hand, the settlement of particles causes the particle concentration in the bottom area to increase, which makes the collision effect between particles in the bottom area of the cylinder stronger.

3.4. *Simulation model validation and analysis*

In order to further demonstrate the reasonableness of the simulation results, we use mean squared error (MSE) and the coefficient of determination (R-squared, R^2) to quantitatively assess the agreement between simulation and experiment. The comparison results are shown in Table 2.

The lower the MSE value, the closer the R2 value is to 1, indicating that the simulation results are more consistent with the

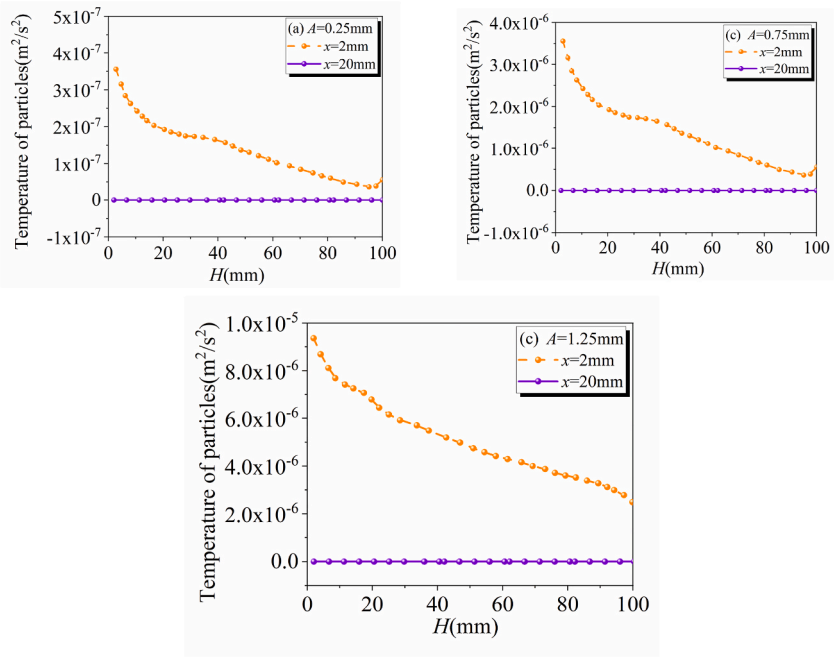

Fig. 11. Effect of the vibration amplitude on the granular temperature under the condition of f = 60Hz

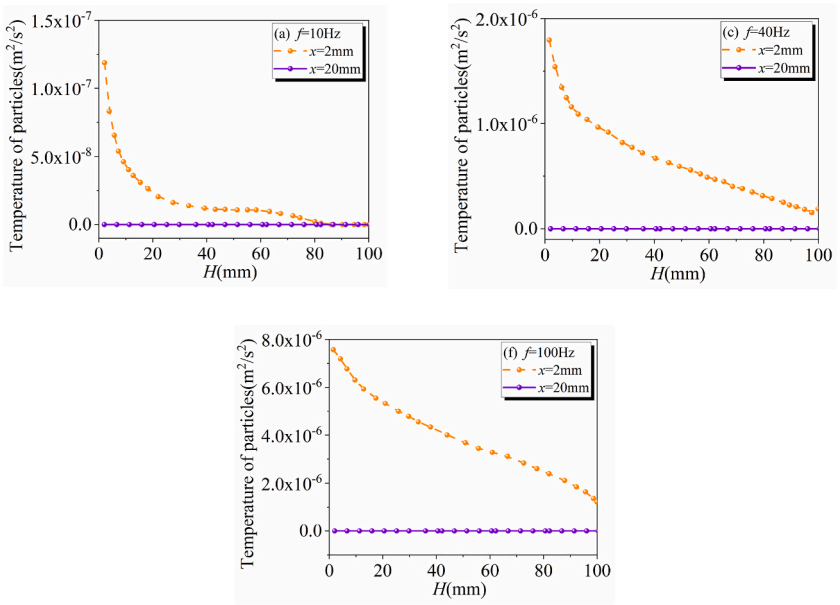

Fig. 12. Effect of the vibration frequency on the granular temperature under the condition of A = 0.75 mm.

experimental data. As can be seen from Table 2, the MSE values of the simulation results in settling rate, concentration propfile and particle velocity are 0.015, 0.021 and 0.012, respectively.These data indicate that the errors between the simulation results and the experimental data in describing the settling rate, concentration profile and particle velocity are relatively small.The values in Table 2 demonstrate the consistency between the simulation results and experimental data. This indicates that the model used is effective in describing and predicting these behaviors.

4. Conclusion

In this study, computational fluid dynamics (CFD) software is mainly used to simulate the motion behaviour of coal particles in CWS under vibration conditions, and the motion of coal particles is mathematically processed through quasi-fluidization of particles, two-fluid model based on the Euler method and external excitation force model. The main conclusions are as follows.

(1) Through the analysis of the settlement results of CWS under static, low vibration intensity and high vibration intensity, it can be seen that without vibration, the coal particles in the CWS gradually settle to the bottom of the container due to the action of gravity only. The CWS concentration shows regular stratification along the simplified height and presents three distinct regions: A low concentration zone at the top of the barrel, a transition zone in the middle, and a high concentration zone at the bottom. When the vibration intensity is low, the excitation force received by the particles is not enough to overcome the action of gravity. The slight vibration energy may activate the motion of the particles, making the particles lose and promoting the settlement under the action of gravity. When the vibration intensity is high, the violent reciprocating motion caused by sinusoidal vibration will cause severe shaking and uncertainty of the container, resulting in the coal particles do not uniformly fall along the axial direction of the container. However, there is back mixing up and down. In the near wall and central area of the cylinder, the concentration of CWS along the height of the cylinder has shown entirely different characteristics from that under static conditions.

(2) When no vibration is added, the motion speed of coal particles is low on the whole, and the movement speed of the top particles is faster than that of the bottom particles; When vibration is applied, the motion velocity of coal particles gradually approaches the sinusoidal motion velocity of the external excitation force. Since the particles at the bottom of the simplified character are the first to be affected by vibration, the vibration energy is further transferred to the top particles through the collision of particles, and the speed of the particles at the bottom is incredible. Low vibration energy will activate the movement of coal particles near the wall and make the movement of coal particles at different radial positions more stable. However, at static and high vibration intensity, the movement of particles in the near-wall area is different from that in the central area due to the obstruction effect of the wall surface on particle movement.

(3) It can be seen from the particle pseudo-temperature study that the particles' temperature in the near-wall area is obviously higher than that in the central area. This is because, in the near-wall area, collisions occur not only between particles but also between particles and the wall surface. In the axial distribution, the temperature of particles in the bottom region is higher, which is on the one hand because the particles in the bottom region move faster, and the collision is more intense. On the other

Table 2
Comparison of MSE and R^2 between simulation results and experimental data.

Parameter	MSE	R^2
Settling rate	0.015	0.92
Concentration profile	0.021	0.88
Particle velocity	0.012	0.94

hand, due to the higher concentration of coal particles in the bottom area, the probability of collision between particles is greater.

(4) Low frequency or low amplitude is conducive to coal particles settling to the bottom of the simplified character. Low vibration intensity can activate the coal particles in the cylinder, and promote the settlement of coal particles under the action of gravity, thus increasing the compactness of coal particles in the bottom area, squeezing water to the top area, resulting in the reduction of the concentration of coal particles in the top area. When the vibration intensity is more significant, the vibration energy is higher, the particles are excited by more significant force, and the movement speed is faster. The reciprocating sinusoidal vibration will aggravate the collision between the particles, which is not conducive to the further compression of the particle group. The concentration of coal particles in the bottom area starts to decline with the further increase of the vibration intensity. At the same time, in the top region, the intensification of particle movement and collision will also lead to partial back mixing or backflow of coal particles, which shows that with the increase of vibration intensity, the concentration of coal particles in the top region gradually increases.

The findings of this research have significant potential applications in the storage and transportation of CWS. The study provides a better understanding of the motion behavior of coal particles under vibration conditions. Therefore, the results of this study can be used as a guideline for the development of efficient and cost-effective CWS transportation systems.

The simulation results show that the MSE values of settling rate, concentration distribution and particle velocity are 0.015, 0.021, 0.012, respectively.These values are relatively low, which implies the consistency between the simulated results and the experimental data. Meanwhile, the R2 values were 0.92, 0.88, and 0.94, respectively, which indicated a high correlation between the simulated settling rate, concentration distribution, and particle velocity and the actual data.

Despite the findings and contributions of this study, there are several limitations that should be acknowledged. Firstly, the results of this study are based solely on the assumptions and simplifications used in the numerical simulations. Although efforts have been made to ensure the accuracy of the simulations, there are still uncertainties and potential errors associated with the modeling assumptions and parameters used. Secondly, the scope of this study is limited to a specific set of conditions and scenarios. Other factors and variables that may affect the results have not been considered. Thirdly, the experimental validation of the numerical simulations was not carried out due to the constraints of time and resources. In addition, the presence of additives in CWS complicates its microstructure. Future studies will extend the simulations to incorporate the effects of additives. The representativeness of the model will be enhanced by capturing the effect of additives on particle behavior, suspension stability, or settling characteristics.

Data availability statement

The labeled dataset used to support the findings of this study are available from the corresponding author upon request.

CRediT authorship contribution statement

Yunfeng Bai: Visualization, Writing – original draft, Data curation, Investigation. **Wenge Song:** Formal analysis, Project administration, Validation. **Xinju Liu:** Resources, Software, Writing – original draft.

Declaration of competing interest

The authors declare that they have no known competing financial interests or personal relationships that could have appeared to influence the work reported in this paper.

Acknowledgments

This work is supported by CHN ENERGY Technology Innovation Project No.GJNY-19-48《The Research and Application of Coal Water Slurry Technology Using Shendong Slime Flotation Clean Coal》.

References

[1] G. Qing, et al., Driving factors of energy consumption in the developed regions of developing Countries: a case of zhejiang province, China, Atmosphere 12 (9) (Sep. 2021) 1196, https://doi.org/10.3390/ATMOS12091196, 2021, Vol. 12, *Page 1196*.

[2] D. Das, R.K. Mohapatra, H. Belbsir, A. Routray, P.K. Parhi, K. El-Hami, Combined effect of natural dispersant and a stabilizer in formulation of high concentration coal water slurry: experimental and rheological modeling, J. Mol. Liq. 320 (2020) 114441, https://doi.org/10.1016/j.molliq.2020.114441.

[3] L.J.R. Nunes, Potential of coal–water slurries as an alternative fuel source during the transition period for the decarbonization of energy production: a review, Appl. Sci. 10 (7) (Apr. 2020) 2470, https://doi.org/10.3390/APP10072470, 2020, Vol. 10, *Page 2470*.
[4] M. Karthikeyan, W. Zhonghua, A.S. Mujumdar, Low-Rank Coal Drying Technologies—Current Status and New Developments, vol. 27, 2009, pp. 403–415, https://doi.org/10.1080/07373930802683005, no. 3.
[5] M.A. Dmitrienko, P.A. Strizhak, Coal-water slurries containing petrochemicals to solve problems of air pollution by coal thermal power stations and boiler plants: an introductory review, Sci. Total Environ. 613 (614) (Feb. 2018) 1117–1129, https://doi.org/10.1016/J.SCITOTENV.2017.09.189.
[6] H.A. Jati, N. Monei, G. Barakos, M. Tost, M. Hitch, Coal Slurry Pipelines: A Coal Transportation Method in Kalimantan, Indonesia, vol. 35, 2021, pp. 638–655, https://doi.org/10.1080/17480930.2021.1949857, no. 9.
[7] K.Y. Vershinina, N.E. Shlegel, P.A. Strizhak, Relative combustion efficiency of composite fuels based on of wood processing and oil production wastes, Energy 169 (Feb. 2019) 18–28, https://doi.org/10.1016/J.ENERGY.2018.12.027.
[8] A. Routray, P.K. Senapati, M. Padhy, D. Das, R.K. Mohapatra, Effect of mixture of a non-ionic and a cationic surfactant for preparation of stabilized high concentration coal water slurry, International Journal of Coal Preparation and Utilization 42 (3) (Mar. 2022) 925–940, https://doi.org/10.1080/19392699.2019.1674843.
[9] E.Y. Shadrin, et al., Coal-water slurry atomization in a new pneumatic nozzle and combustion in a low-power industrial burner, Fuel 303 (Nov. 2021) 121182, https://doi.org/10.1016/J.FUEL.2021.121182.
[10] Z. Xue, Y. Gong, Q. Guo, F. Wang, G. Yu, Visualization study on breakup modes of coal water slurry in an impinging entrained-flow gasifier, Fuel 244 (May 2019) 40–47, https://doi.org/10.1016/J.FUEL.2019.01.186.
[11] Y. Lu, et al., Effect of concentration, size, granularity, shear time and temperature on rhological properties of coal water slurries, IOP Conf. Ser. Mater. Sci. Eng. 1126 (1) (Mar. 2021) 012027, https://doi.org/10.1088/1757-899X/1126/1/012027.
[12] B. Cheng, R. Chang, Q. Yin, J. Li, J. Huang, H. Chen, A PSR-AHP-GE model for evaluating environmental impacts of spoil disposal areas in high-speed railway engineering, J. Clean. Prod. 388 (Feb. 2023) 135970, https://doi.org/10.1016/J.JCLEPRO.2023.135970.
[13] H. Zhao, et al., Influence of rheological properties on air-blast atomization of coal water slurry, J Nonnewton Fluid Mech 211 (Sep. 2014) 1–15, https://doi.org/10.1016/J.JNNFM.2014.06.007.
[14] J. Liu, J. Wang, C. Chen, Y. Chen, X. Zheng, Preparing coal slurry from organic wastewater to achieve resource utilization: slurrying performance and dispersant suitability, Fuel (2022) 126970, https://doi.org/10.1016/J.FUEL.2022.126970.
[15] Y. Zhang, et al., Performance and mechanism of polyacrylamide stabilizers in coal water slurry, Colloids Surf. A Physicochem. Eng. Asp. 630 (2021) 127544, https://doi.org/10.1016/J.COLSURFA.2021.127544.
[16] R.K. Mohapatra, D. Das, M. Azam (Eds.), Chemical Modification of Solid Surfaces by the Use of Additives, BENTHAM SCIENCE PUBLISHERS, 2021, https://doi.org/10.2174/9789815036817210101.
[17] R.K. Mohapatra, D. Das, M. Azam (Eds.), Chemical Modification of Solid Surfaces by the Use of Additives, BENTHAM SCIENCE PUBLISHERS, 2021, https://doi.org/10.2174/9789815036817210101.
[18] T. Norton, D.W. Sun, J. Grant, R. Fallon, V. Dodd, Applications of computational fluid dynamics (CFD) in the modelling and design of ventilation systems in the agricultural industry: a review, Bioresour. Technol. 98 (12) (Sep. 2007) 2386–2414, https://doi.org/10.1016/J.BIORTECH.2006.11.025.
[19] F.D. Witherden, A. Jameson, Future directions of computational fluid dynamics, in: *23rd* AIAA Computational Fluid Dynamics Conference, vol. 2017, 2017, https://doi.org/10.2514/6.2017-3791.
[20] P.v. Sivaprasad, N. Girase, S. Sarkar, O. Wijk, Role of modelling in the development of high performance steels for important engineering applications, Adv Mat Res 794 (2013) 493–501, https://doi.org/10.4028/WWW.SCIENTIFIC.NET/AMR.794.493.
[21] W. Jeong, J. Seong, Comparison of effects on technical variances of computational fluid dynamics (CFD) software based on finite element and finite volume methods, Int. J. Mech. Sci. 78 (Jan. 2014) 19–26, https://doi.org/10.1016/J.IJMECSCI.2013.10.017.
[22] F.N. Fard, B. McLaury, S. Shirazi, Effect of Cell Size on Particle-Eddy Interaction and Erosion Predictions Using Commercial CFD Software (FLUENT), vol. 1, American Society of Mechanical Engineers, Fluids Engineering Division (Publication) FEDSM, 2013, pp. 1287–1295, https://doi.org/10.1115/FEDSM2012-72294, no. PARTS A AND B.
[23] A. Rheinländer, U. Leser, G. Graefe, Optimization of complex dataflows with user-defined functions, ACM Comput. Surv. 50 (3) (May 2017), https://doi.org/10.1145/3078752.
[24] M. Elkarii, R. Boukharfane, S. Benjelloun, and C. Bouallou, "Particulate Science and Technology A CFD-Based Surrogate Model for Predicting Slurry Pipe Flow Pressure Drops A CFD-Based Surrogate Model for Predicting Slurry Pipe Flow Pressure Drops", doi: 10.1080/02726351.2022.2110341.
[25] S. Kuharat, O. Anwar Bég, A. Kadir, M.D. Shamshuddin, Computational study of heat transfer in solar collectors with different radiative flux models, Heat Tran. Asian Res. 48 (3) (May 2019) 1002–1031, https://doi.org/10.1002/HTJ.21418.
[26] S.M. Hasheminejad, A.H. Rabiee, H.R.T. Bahrami, Active closed-loop vortex-induced vibration control of an elastically mounted circular cylinder at low Reynolds number using feedback rotary oscillations, Acta Mech. 229 (1) (Jan. 2018) 231–250, https://doi.org/10.1007/S00707-017-1960-Y/METRICS.
[27] M. Esmaily, J.A.K. Horwitz, A correction scheme for two-way coupled point-particle simulations on anisotropic grids, J. Comput. Phys. 375 (Dec. 2018) 960–982, https://doi.org/10.1016/j.jcp.2018.09.009.
[28] E. Kirkinis, Null-divergence nature of the odd viscous stress for an incompressible liquid, Phys Rev Fluids 8 (1) (Jan. 2023) 014104, https://doi.org/10.1103/PHYSREVFLUIDS.8.014104/FIGURES/5/MEDIUM.